International Journal of Physical Sciences

Volume 10 Number 10 30 May, 2015

ISSN 1992-1950

Academic Journals

ABOUT IJPS

The **International Journal of Physical Sciences (IJPS)** is published weekly (one volume per year) by Academic Journals.

International Journal of Physical Sciences (IJPS) is an open access journal that publishes high-quality solicited and unsolicited articles, in English, in all Physics and chemistry including artificial intelligence, neural processing, nuclear and particle physics, geophysics, physics in medicine and biology, plasma physics, semiconductor science and technology, wireless and optical communications, materials science, energy and fuels, environmental science and technology, combinatorial chemistry, natural products, molecular therapeutics, geochemistry, cement and concrete research, metallurgy, crystallography and computer-aided materials design. All articles published in IJPS are peer-reviewed.

Contact Us

Editorial Office: ijps@academicjournals.org

Help Desk: helpdesk@academicjournals.org

Website: http://www.academicjournals.org/journal/IJPS

Submit manuscript online http://ms.academicjournals.me/

Editors

Editorial Board

International Journal of Physical Sciences

Table of Contents: Volume 10 Number 10, 30 May, 2015

ARTICLES

academicJournals

Vol. 10(10), pp. 329-334, 30 May, 2015
DOI: 10.5897/IJPS2014.4205
Article Number: 83973DE53641
ISSN 1992 - 1950

http://www.academicjournals.org/IJPS

International Journal of Physical Sciences

Full Length Research Paper

Oscilating magnetic field an anti malaria therapy

Abajingin David Dele

Department of Physics and Electronics, Adekunle Ajasin University, Akungba-Akoko, Ondo-State, Nigeria.

Received 3 September, 2014; Accepted 13 January, 2015

The effect of oscillating magnetic fields (OSMF) on malaria infected albino rats of about three weeks old was investigated. Ten malaria parasite - infected rats were obtained from the Department of Parasitology, University College Hospital Ibadan. The rats were randomly divided into an experimental and a control groups, of five animals each. The rats in the experimental group were exposed to OSMF of 41mT for fourteen consecutive days after fourteen days of acclimatization. Results obtained from the experimental group showed that the level of the pack cell volume (PCV) gradually increased during exposure whereas the parasitamial level (PD) decreased. Results from the control group showed that the level of the PCV decreased significantly and that of the parasitamial level (PD) increased significantly over time. The results suggest that malaria could be cured with the use of OSMF,

Key words: Oscillating magnetic field, *Plasmodium falciparium*, *Plasmodium vivax*, *Plasmodium ovale*.

INTRODUCTION

In recent years, there has been an increase in reported cases of ineffectiveness of anti-malaria drugs, which is traced to the resistance of malaria parasite (Plasmodium) to the drugs (Jean et al., 1999). In Nigeria, this has been traced to persistent use of adulterated anti-malaria drugs, (Akuyili, 2005). The ineffectiveness of the available anti-malaria drugs has led to the use of combination therapy, which is the spontaneous administration of two to three malaria drugs at a time (Feng et al., 2003). The increase in reported emergence of multiple resistances of the malaria parasites to this mode of therapy has increased the urgency of need of an alternative strategy for destroying malaria parasites. This is in essence the main aim of this study.

Malaria is a vector borne infectious disease caused by protozoan parasite of the genus plasmodium. Only four types of the parasite can affect humans. These are the *Plasmodium falciparium, Plasmodium vivax,* and *Plasmodium ovale,* and *Plasmodium malariae* (Alex, 2001). *P. falciparum* is the most common cause of infection and responsible for about 80% of all the severe malaria cases. It is also responsible for about 90% of the death from malaria. *P. vivax* and *P. ovale* are responsible for chronic malaria infection. These Plasmodia reside and develop to a full stage within the liver and stream into the blood system. Thus the immediate malaria diseases associated with the *P. vivax* and *P. ovale* in any other organ of the body is not yet known.

P. falciparium in full development within the blood has been observed to feed on the globin part of the hemoglobin, the pigment found in red blood cells. The iron-containing heme portion of hemoglobin is left intact within the parasite. Heme is very toxic to the *P. falciparium*. In order to eliminate the toxic effects of the free heme, *P. falciparium* binds the heme together into a polymer called hemozoin whichacts essentially like a tiny

E-mail: abajingindd@yahoo.com

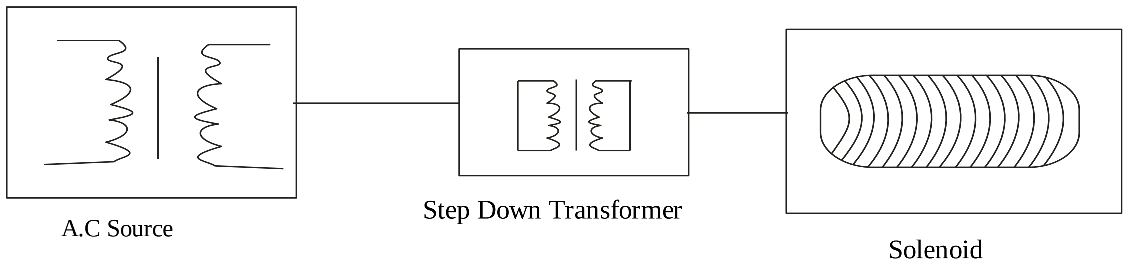

Figure 1. Schematic diagram showing the block diagram of the connection of the AC power source, the step down transformer and the solenoid.

bar magnet, (Henry, 2000). Hemozoin is not toxic, thus aids the existence of the plasmodium parasite in the blood.

The discovery of Henry (2000) suggested that a possible cure to malaria infection as caused by *P. falciparium* parasite may be obtained if a toxic environment due to the hemes can be maintained within the blood. This can be achieved if an external device can be put in place to break up the tiny bar magnets (HERMOZOINS) formed by the *P. falciparium* parasite back into heme as they are formed and thus renders the blood environment toxic to the Plasmodium parasites. With this background, this study is set to examine the effects of oscillating magnetic field on the hemozoins formed by the *P. falciparium* parasite.

MATERIALS AND METHODS

Animals

Ten malaria parasite-infected with *P. falciparium* albino rats of about 2 to 3 weeks old and of average weight of about 65 g were used for this study. These rats were obtained from the Department of Parasitology University College Hospital (UCH), Ibadan, Nigeria.

Materials

The materials used for this study are: a solenoid, a wooden cage kept in the animal house of the Adekunle Ajasin University, cereal pellet and 12 V step down transformer. The solenoid is an electrical device generally used to generate magnetic field. It is constructed from a cylindrical wooden frame of length 0.615 m, with a diameter 0.595 m, on which 2950 turns of coil of 0.05 mm diameter copper wire is wound. An alternating current power source (AC) is connected to the solenoid through a 12 V step down transformer, which helps to produce an AC current output of 5.50A, (Figure 1).

Procedures of experiment

Ten albino rats of about 2 to 3 weeks old and of an average weight of 65 g infected with malaria parasite were used for this study. These rats were housed in a wooden cage at room temperature (25 to 27°C) maintained in a normoxic condition for 2 weeks under a 12 h-light-dark cycle. They were fed regularly with a standard cereal pellet and water for two weeks. This two week period was meant to ascertain full maturation of the malaria parasite in the rats. Two of the rats were found to be too weak for the experiment and died on the fifth day. Blood samples from the rats were taken at a day interval for the two weeks. The samples were put in an anticoagulant bottle and taken to Adekunle Ajasin University Health Centre for parasite growth investigation. The weight of each rat was taken every three days. After these first two weeks, the rats were randomly divided into an experimental and a control group, each group contained four rats. The rats in the experimental group were all placed in the solenoid where they were exposed to the OSMF of 41mT, 10 h per day for fourteen consecutive days at the sametime.

Blood samples of rats in the experimental and control groups were again taken every other day and on the last day of the experiment after each exposure. Parasite growth in the blood was investigated.The sampled blood from the rats was observed under a microscope with high resolving power. The observation for the degree of parasitamia (PD) from the microscope was classified as:

(i) 5 to 10% of cells were parasitized and symbolized as +
(ii) 10 to 20% of cells were parasitized and symbolized as ++
(iii) 20 to 30% of cells were parasitized and symbolized as +++.

These (PD) as expressed this way shows the level of the malaria parasite expressed by the number of plus signs. The packed cell volume (PCV) percentage calculation of the blood sample was obtained using the expression:

$$PCV = \frac{W.B.C}{Total\ Packed\ Cell} \quad (1)$$

Where W.B.C is the white blood cell count.

RESULTS AND DISCUSSION

The average weights of the rats in the experimental and control groups before exposure to OSMF are shown in Figure 2. The curves show that for the first five days of acclimatization, the rats fed well on the pellets provided as a result the average weight of the rats increased and they are very active. From the fifth day the average weight of the rats decreased and there activity level also decreased.

Values of PCV and PD before exposure to OSMF of the rats in the two group are put together in Tables 1 and 2. Table 1 shows the calculated values of PCV of the blood samples of each of the four rats for the rats in the

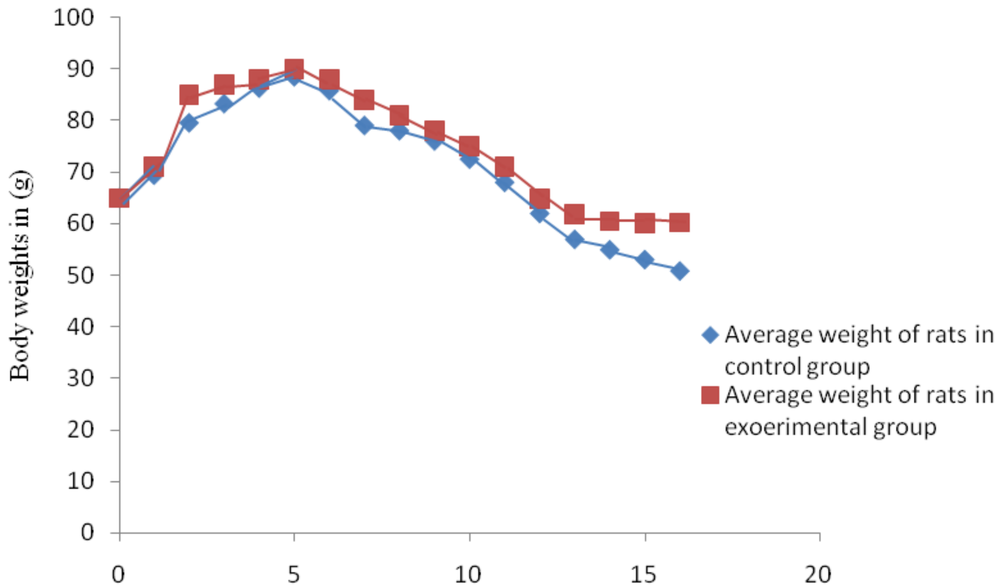

Figure 2. Variation of average body weight of the rats in the both control and the experimental groups exposure to OSMF.

Table 1. Calculated values of the PVC and PD for each of the rats in the control group for the first fourteen days.

Animal	1stBlood Sample		2nd Blood Sample		3rdBlood Sample		4th Blood Sample		5th Blood Sample	
	PD	PCV (%)	PD	PCV (%)	PD	PCV (%)	PD	PCV (%)	PD	PCV (%)
1st Rat	++	42	+++	36	+	31	+	27		21
2nd Rat	++	38	++	30	+	27	+	21		12
3rd Rat	++	32	+	27	+	22	+	18	+++	12
4th Rat	++	41	+	32	-	23	+	15		13

control group. They changed from 42 to 21%, 38 to12%, 32 to 12% and 41 to 13%, during the period, all in downward trend. Since these values were computed from Equation (1), this downward trend in the values of the PCV was attributed to the decrease in white blood cells. Evidently the red blood cells have greatly reduced by the attack of the hemoglobin by malaria parasite. This we believe has adversely affected the eating habit of the rats, and thus the appreciable decrease in the weight of the rats. The graphical variation of the PCV of the control rats with days of acclimatization is shown in Figure 3.

In Table 2, the calculated value of PCV of the blood samples of each of the four rats in the experimental group,showed changes vary from 48 to 18%, 35 to 17%, 40 to 14% and 36 to 13%, all again in the downward trends. The graphical variation of the PCV of the rats in the experimental group with number of days is shown in Figure 4.

Table 3 contains the calculated values of PCV from the blood samples obtained after a 10 h exposure to OSMF of the rats in the experimental group during exposure. The variation of the PCV with number of days for each rat is shown in Figure 5.

The first column in Table 3 contains the calculated values of PCV and PD of the blood samples collected from each rat in the experimental group on the first day of treatment (exposure). This coincides with the day when the last values of the PCV and PD for the rats before they were exposed to OSMF. There was no marked difference in PCV and PD between these values in first column of Table 3 and those in column four in Table 2. The first rat of the experimental group showed an increase PD after the fourth day of exposure, with PCV rising to 37%. The PCV of the second, third and fourth rats remarkably increased to 29, 30 and 22% respectively. This is an indication that the number of the malaria parasites has decreased in these rats. The trend changed as from the eight day as the values of the PCV for all the four rats respectively assumed constant average values of 40, 37, 31 and 41%. Consequently, there was a rapid decrease in the PD reported for all the experimental rats within this period, (8th to 14th days).

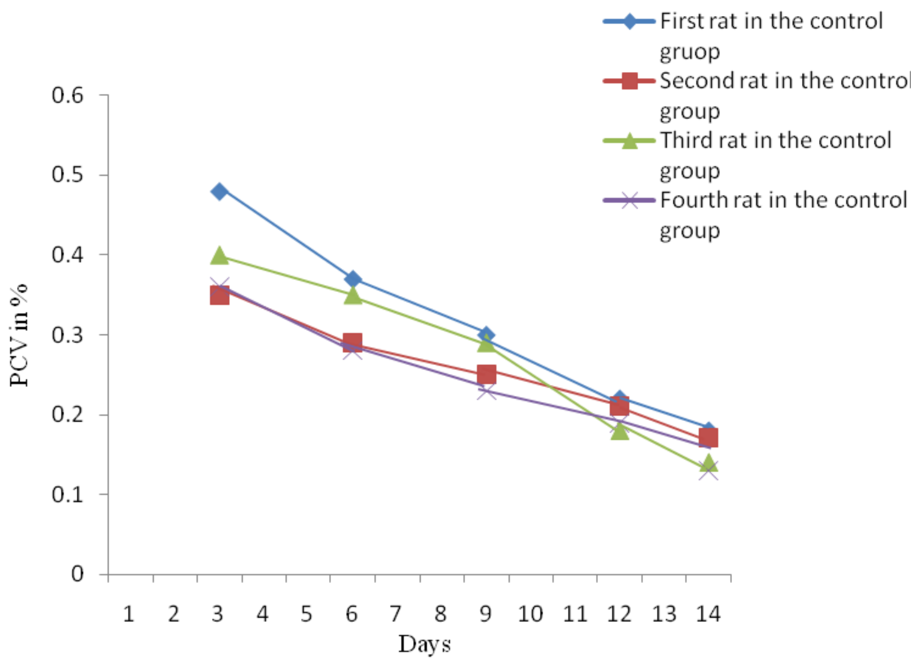

Figure 3. Variation of the PCV of rats in the control group against the number of days.

Table 2. Calculated values of the PVC and PD for each of the rats in the experimental group before exposure to OSMF after two weeks.

Animal	1st Blood sample		2nd Blood sample		3rd Blood sample		4th Blood sample		5th Blood sample	
	PD	PCV (%)	PD	PCV (%)	PD	PCV (%)	PD	PCV (%)	PD	PCV (%)
Rat 1	+	48	++	37	+++	30	+++	22	++++	18
Rat 2	++	35	++++	29	++++	25	++++	21	++++	17
Rat 3	+	40	++	35	++++	29	++++	18	+++	14
Rat 4	+	36	+++	28	++++	23	++++	19	++++	13

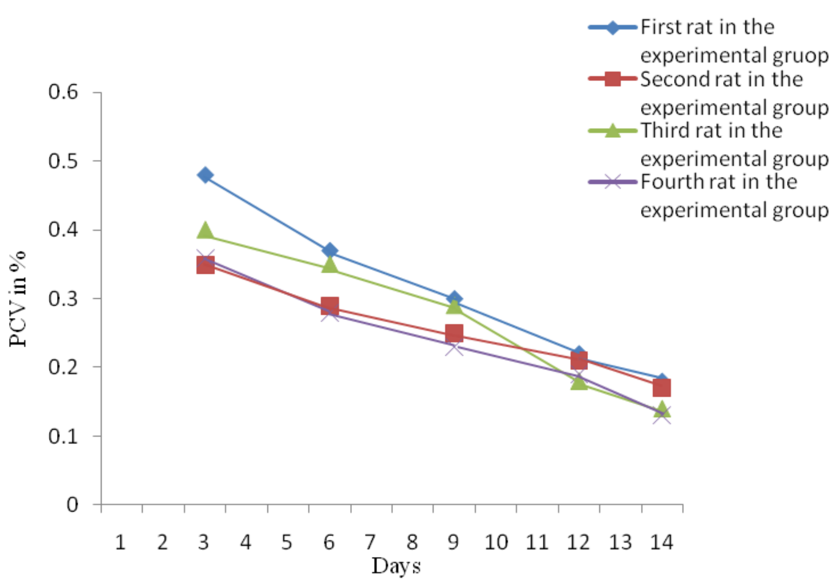

Figure 4. Variation of the PCV of rats in the experimental group against the number of days before exposure to OSMF.

Table 3. Calculated values of the PVC and PD for each of the rats in the experimental group after a 10 h exposure to OSMF for two weeks.

Animal	1stBlood sample		2nd Blood sample		3rdBlood sample		4th Blood sample		5th Blood sample		6th Blood sample		7th Blood sample	
	PD	PVC (%)	PD	PCV (%)	PD	PVC (%)	PD	PCV (%)	PD	PCV (%)	PD	PCV (%)	PD	PCV (%)
Rats 1	++	18	++	37	+	42	+	41	+	40	+	40	+	40
Rats 2	++	17	++	29	++	37	+	38	+	38	+	38	+	37
Rats 3	+	14	++	30	++	32	+	31	+	39	+	31	+	31
Rats 4	+	13	++	22	++	37	+	41	+	40	+	40	+	41

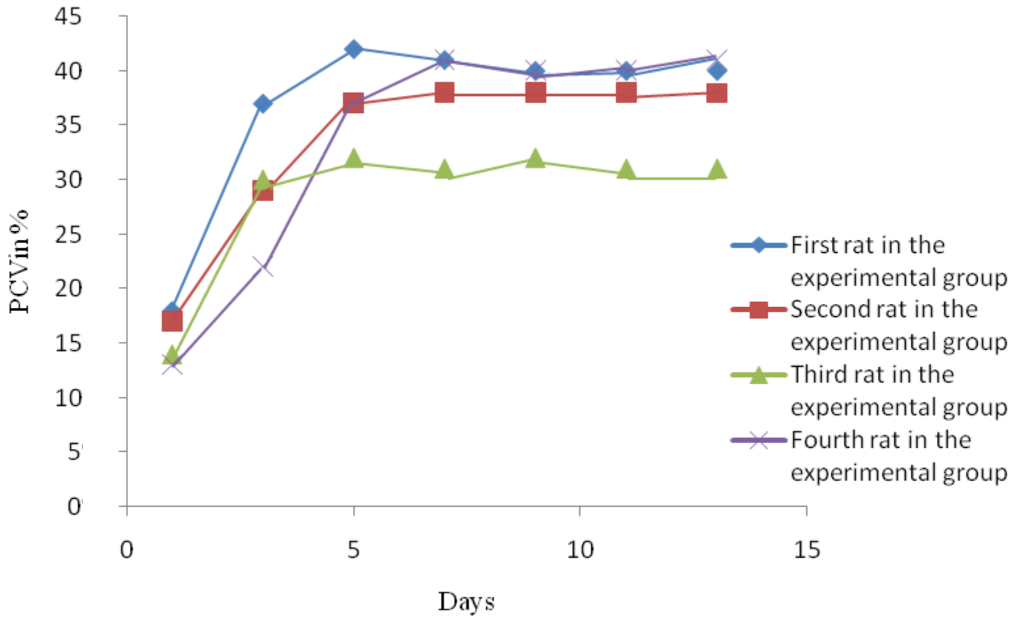

Figure 5. Variation of the PCV of rats in the experimental group after 10 h each day exposure to OSMF.

Table 4. Calculated values of the PCV and PD for each of the rats in the control group after the first two weeks of acclimatization.

Animal	1stBlood Sample		2nd Blood Sample		3rdBlood Sample		4th Blood Sample		5th Blood Sample		7th Blood Sample	
	PD	PVC (%)	PD	PCV (%)	PD	PVC (%)	PD	PCV	PD	PCV	PD	PCV
1ST Rat	++	21	++	15	+++	09	----	---	-----	---	----	---
2nd Rat	++	12	+++	07	+++	---	----	---	-----	---	----	---
3rd Rat	+	12	+++	06	++	---	----	---	-----	---	----	---
4th Rat	+	13	+++	06	++	---	----	---	----	---	----	---

Table 4 contains the calculated values of PCV and PD for the control group after the first two weeks of acclimatization. The calculated values of the PCV decrease rapidly to a very negligible values when the third blood sample was taken after the first fourteen days of acclimatization for the first rat, while this rapid decrease was observed in the second sample for other rats. The measure PD equally increased. The four rats were very weak at this instance and they eventually died after the third blood samples were taken from them. For this reason, PCV and PD values were not obtained after that time.

Conclusion

The main aim of this study was to investigate an alternative therapy for malaria using an external agent which can successfully be used to separate the hemozoin into the hemes so that a toxic environment is maintained within the blood as long as the malaria parasite are present in the blood stream of the host. The results from this study have shown that an oscillating magnetic field can be used for this purpose. The curative effect obtained through the use of OSMF suggests a parallel or an alternative malaria therapy to the orthodox medical antimalarial therapy. Although a possible cure for malaria issuggested at this stage, this cannot be said to be a conclusive study as a post exposure observation of the rats is required to ascertain that the malaria parasites are not just rendered dormant for a period of time and would become active again when the oscillating magnetic field is removed. Also, it is necessary to find out the extent of damages the OSMF could cause to tissues of the body where the malaria parasite resided.

Conflict of Interest

The authors have not declared any conflict of interest.

REFERENCES

Akuyili D (2005). Imported Drug: Nigeria Scenario. Published in The Nation, July 10. 1(0345):3.

Alex SR (2001). Production of Hemozoins in Malaria Infested Rats. Unpublished Research Work sited in www. By Research Team Work on Hemozoins at the Vanderbilt University, U.S.A.

Feng X, Joy D, May J (2003). Early origin of resent expansions of *Plasmodium falciparum*. Science 300(5617):318-321.

Henry L (2000). Magnetic field may hold key to malaria treatment. A symposium paper in the website, http://www.washington.edu/nwes/2000/30.

Jean EF, Michelle AW, Ceon R, Henry CL (1999). Magnetic Fields and Malaria. Kluwer Academic Publishers, MA, pp. 343-349.

academicJournals

Vol. 10(10), pp. 335-341, 30 May, 2015
DOI: 10.5897/IJPS12.684
Article Number: 705D42D53644
ISSN 1992 - 1950

http://www.academicjournals.org/IJPS

International Journal of Physical Sciences

Full Length Research Paper

Computational analysis of the effective parameters on two-phase bubbly water flow in a ramjet propulsion system

J. Hosseini[1], M. Sefid[2]* and S. Niazi[1]

[1]University of Hormozgan, Bandar Abbas, Hormozgan, Iran.
[2]University of Yazd, Yazd, Iran.

Received 30 October, 2012; Accepted 16 April, 2015

A computational study of the flow field characteristics and the performances of two-phase bubbly flow in water jet of a ramjet propulsion system with a diverging-converging nozzle has been performed. The analysis use a finite volume approach for the main flow coupled numerically with the Lagrangian equations for the bubbles motion including the change of bubbles radii with time. Computed results for an experimental two-phase flow in a ramjet propulsion system with a converging-diverging nozzle are presented to validate the numerical model. The performance of the ramjet for different initial velocities of the incoming water and for various locations of the bubbles injections has been studied. Results reveal that the best location for the bubbles injection is at the beginning of the nozzle section and produces a higher thrust.

Key words: Bubble dynamic, water ramjet, thrust, computational fluid dynamics (CFD), two-phase flows.

INTRODUCTION

Considerable interest exists in the engine community in investigating two-phase bubbly flows in waterjet of a ramjet, experimentally, or numerically. This is due to the performance and interactions of the bubbles on the flow and augmenting the ramjet propulsion thrust. In the marine ramjets the water flow enters the ramjet from a diffuser which causes the velocity reduction and pressure increase based on Bernoulli equation. The high pressure flow from the diffuser enters the mixing chamber where the bubbles are injected into the water and after that enters the nozzle. In the nozzle the pressure decrease and the bubbles accelerate the water velocity and this increasing velocity at the nozzle exit creates a higher value for the thrust.

Computational fluid dynamics (CFD) methods provide an efficient way of investigating the complex flow phenomena within two-phase flows in ramjet propulsion systems. In addition, due to the availability of post-processing and scientific visualization software, the computed flow field can be extensively analyzed. It is also convenient to test within numerical model various control strategies, such as energizing of incoming flow using jets.

The earliest studies on bubbly water jets were

*Corresponding author. E-mail: PMmhsefid@yahoo.com

performed by Witte, who proposed the high pressure gas injection in water flow of a propulsion system (Witte, 1969). Amos and Maxwell presented the numerical simulations of an air-augmented waterjet (Amos et al., 1973; Maxwell et al., 1975). A theoretical study on the characteristics of two-phase bubbly water ramjet propulsion was performed by Varshay and Gany (1997). The detailed investigation of the flow field and ramjet performance was presented by Mor and Gany (1997). AleHossein and Qin (2007), numerically simulated the cavitating water jets using Rayleigh-Plesset. Chahine et al. (2008) performed the study of bubble-augmented water jet propulsion system of two phase model development and also constructed experimental validations. Chahine (2008) also investigated the effects of the void fraction on the performance of the bubbly ramjet. Fu et al. (2009) predicted the flow field and the produced thrust of a two-phase bubbly ramjet with converging-diverging nozzle using computational fluid dynamic approach. These three section for the physical processes including the diffuser, mixing chamber, and nozzle and construct separate mathematical models for these sections.

Most numerical studies on the bubbly two-phase water ramjet have been limited to one or two dimensional flow field. In this paper a three dimensional simulation of two-phase bubbly water flow ramjet propulsion system with a converging-diverging nozzle is presented. The model solves the Time-Averaged Navier-Stokes equations for the main water flow using finite volume approach coupled with Lagrangian equations for the bubbles. The paper is organized as follows. At first, governing equations and numerical formulations are described. Next, validation results in the form of velocity and pressure distributions against an experimental two-phase bubbly water flow ramjet are presented. Finally, the effects of various incoming water velocities and the effects of locations of the bubble jets injections on the thrust augmentation are presented.

NUMERICAL FORMULATIONS

In this study, three sets of equations have been considered. First, the time-averaged Navier-Stokes equations including the continuity, and momentum equations have been applied into the water mixed flow, which are:

$$\frac{\partial \rho_m}{\partial t} = div(\rho_m u_m) \tag{1}$$

$$\rho_m \frac{D u_m}{Dt} = -\nabla p_m + \nabla\{2\mu_m \delta_{ij} + \lambda_m(\nabla . \boldsymbol{u}_m)\} \tag{2}$$

Where $\lambda_m = -\frac{2}{3}\mu_m$

The mixture density and viscosity for a void volume fraction α can be shown by:

$$\rho_m = \alpha\rho_b + (1-\alpha)\rho_f \tag{3}$$

$$\mu_m = \alpha\mu_b + (1-\alpha)\mu_f \tag{4}$$

Where the void fraction, α, is defined as the volumes of the bubbles in a cell divided by the volume of that cell:

$$\alpha = \frac{\sum \pi * d_n{}^3/6}{V} \tag{5}$$

The second set of the equation is related to the bubbles motion and trajectory has been derived by Johnson and Hsieh (1966) which is:

$$\frac{du_b}{dt} = F_D(u-u_b) + \frac{\rho}{\rho_b}\frac{3R^{\cdot}}{2R}(u-u_b) + \frac{\rho}{\rho_b}u_b\frac{\partial u}{\partial x} + \frac{1}{2}\frac{\rho}{\rho_b}\left(\frac{du}{dt} - \frac{du_b}{dt}\right) + \frac{(\rho_b-\rho)}{\rho_b}g + \frac{2.594\nu^{1/2}\rho d_{ij}}{\rho_b R(d_{lk}d_{kl})^{1/4}}(u-u_b) \tag{6}$$

Where $F_D = \frac{18\mu}{4\rho_b R_b{}^2}\frac{C_D Re}{24}$

Here the drag coefficient iscalculated by (Haberman and Morton, 1953):

$$C_D = \frac{24}{\text{Re}}\left(1 + 0.197\,\text{Re}^{0.63} + 2.6\times10^{-4}\,\text{Re}^{1.38}\right)$$

$$Re = \frac{2R\rho\left|u - u_b\right|}{\mu} \tag{7}$$

Finally, the third set of the equations computes the changes of the bubble radii using the Rayleigh-Plesset equation:

$$R\ddot{R} + \frac{3}{2}\dot{R}^2 = \frac{1}{\rho}\left[P_v(T_\infty) + P_{G0}\left(\frac{R_0}{R}\right)^{3k} - P - \frac{2\gamma}{R} - \frac{4\mu}{R}\dot{R}\right] + \frac{1}{4}(u - u_b)^2 \tag{8}$$

To specify the bubble behavior the Rayleigh-Plesset equation and the bubble motion tracking should be solved simultaneously. In this paper these equations have been solved using Range-Kutta fourth order equations.

Solution algorithm

To study full 3-D two-way interactions, the void fraction is defined in the 3-D space. The bubble number and size in each α-cell are used to compute the void fraction. The procedure for these unsteady computations is as follows:

1. Initialize the flow field, e.g., from steady state solution of liquid only without considering the bubbles effects using time-averaged Navier-Stokes Equations (1) and (2), or from a known initial solution. The solutions are being used for the bubbles dynamic motions.
2. Allow the bubbles to diffuse one time step in the flow field following injection.
3. According to the bubble size and location resulted from previous step, compute the void fraction using Equation (5).
4. Calculate the mean mixture density and viscosity, $\rho_m(x,y,z,t)$ and $\mu_m(x,y,z,t)$, respectively.
5. Solve the flow field including velocity and pressure distributions with the updated mean mixture density, and proceed to the next time step.
6. Repeat from Step 2 to 5 until reaching the desired time.

Configuration and computational grid

The configuration which was used by Chahine has been chosen as

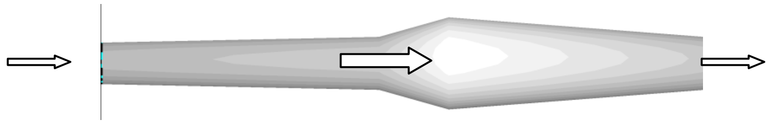

Figure 1. The ramjet nozzle configuration.

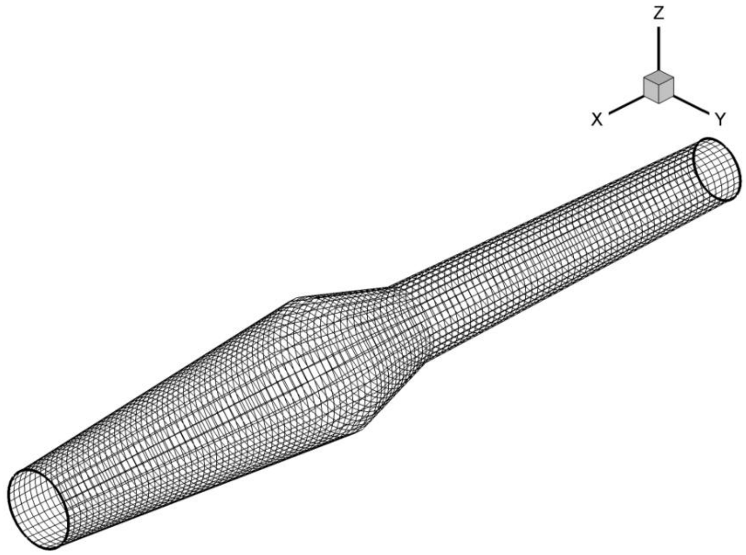

Figure 2. Computational grid.

a reference study to validate the results of the present study. Figure 1 shows the nozzle configuration of the ramjet. A bubble injector is placed at the end of diffuser. Velocity of water at the inlet and the exit pressure are 8 m/s and 1 atm, respectively. Also shown in Figure 2 is the corresponding computational grid used to model the two-phase water flow. The dimensions of the grid are 30 × 40 × 175 in the radial, circumferential, and axial directions, respectively.

RESULTS AND DISCUSSION

For validation purposes, the numerical model was first applied to two-phase bubbly water flow studied experimentally and theoretically by Chahine (2008). To illustrate convergence trend, the radius changes with time of a bubble injected is shown in Figure 3. Initial radius of this bubble is 5 mm and it is injected at pressure 2 atm. Since the pressure inside the nozzle at the injection location is lower than the injection pressure, the bubble expands after the injection and then oscillates with time which finally reaches to a constant value, as illustrated in Figure 3.

Figure 4a and b depict the axial velocity distribution and velocity contour plot on the center line and center plane of the nozzle, respectively. The velocity inside the nozzle decreases with increasing the cross sectional area up to the bubble injector, as it is expected, and then increases

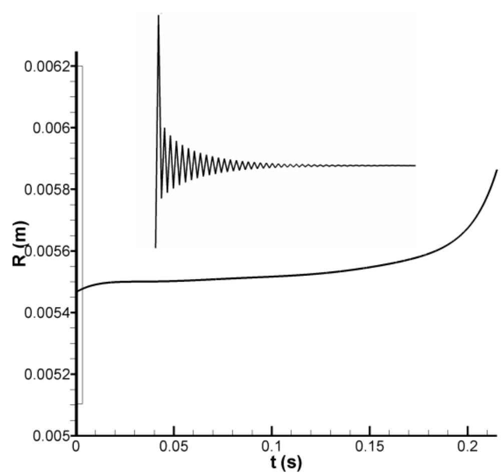

Figure 3. Change of bubble radius with time.

toward the exit plane. In the vicinities of the injected bubbles velocity can exceed the inlet velocity unlike the situation in which air is absent. The axial velocity reaches the value of 13.8 m/s which is higher than the exit velocity of the water without bubbles. The computed results are in good agreement with the Chahine data. Figure 5a

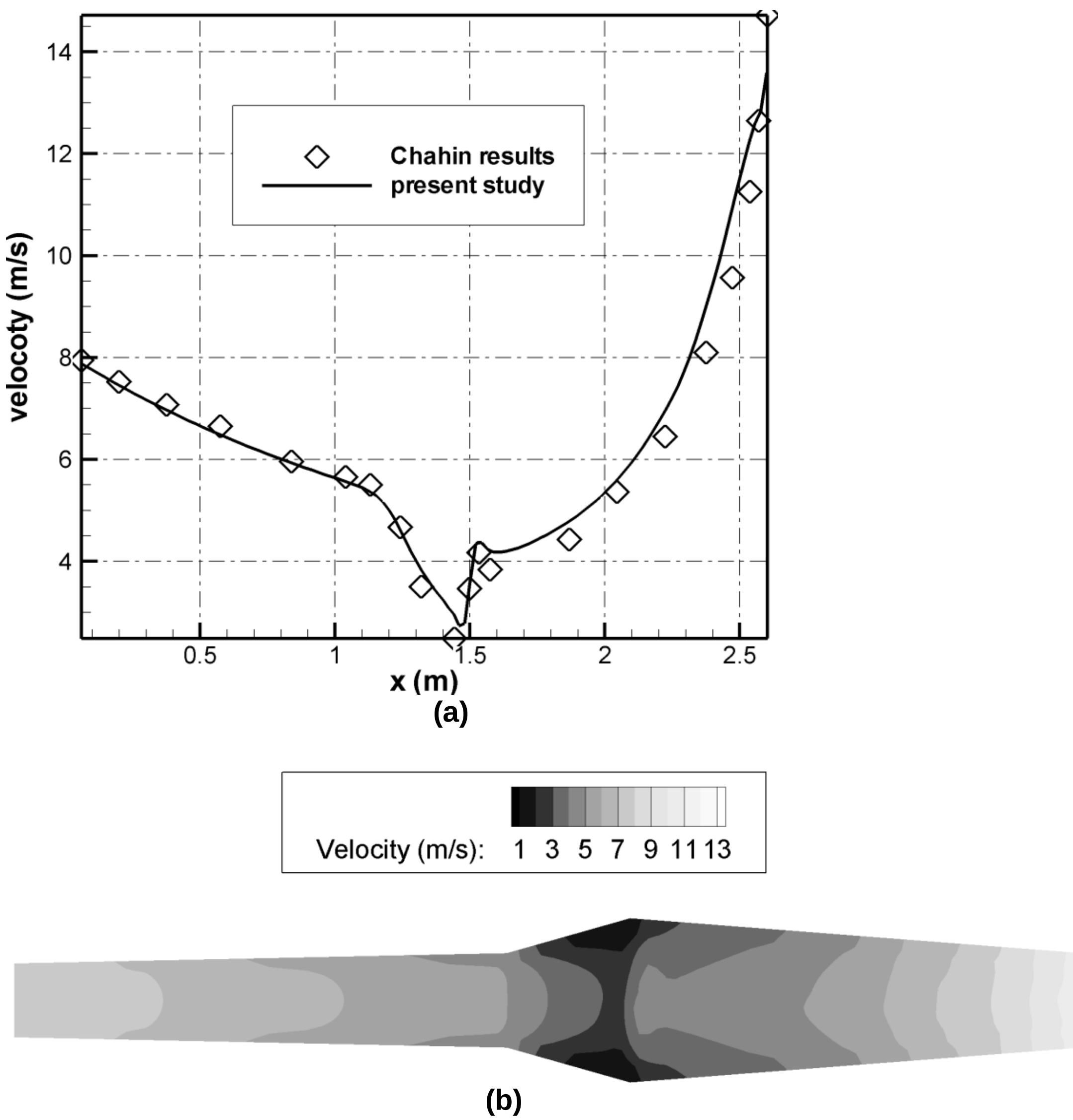

Figure 4. (a) Axial Velocity on the centerline; (b) contour of axial velocity on center plane of ramjet.

shows the pressure profile on the center line, and the pressure distribution on the center plane of the nozzle is presented in Figure 5b. As illustrated in Figure 5a, the corresponding pressure reaches to its maximum value just downstream of the bubble injector. The comparison of pressure distribution obtained from this study shows good agreement with previous studies, too.

Figure 6 shows the void fraction variation inside the nozzle if a set of bubbles were injected at x=1.5 m. It is zero before injection occurs. Then it suddenly rises just after the injection point. It then rises gradually till the outlet due to the pressure drop along the nozzle. Effect of void fraction on velocity distribution in the nozzle also investigated in this study. Figures 7 and 8 show the results for velocity and pressure distribution along the axis of ramjet for two different initial void fractions. It is clear that injection increases the axial velocity and velocity at the outlet is much higher in comparison with water only flow. Also as expected, it is observed that pressure increases at the inlet of ramjet after bubble injection.

Thrust of the nozzle

The main part of this study is to detect the effects of initial incoming water velocity and the positions of the bubbles injections on the performance and the thrust of the ramjet. The thrust equation of the nozzle has two main parts; momentum term and pressure term. Consider a control volume that contains the nozzle. The thrust can be computed by integrating the pressure and the

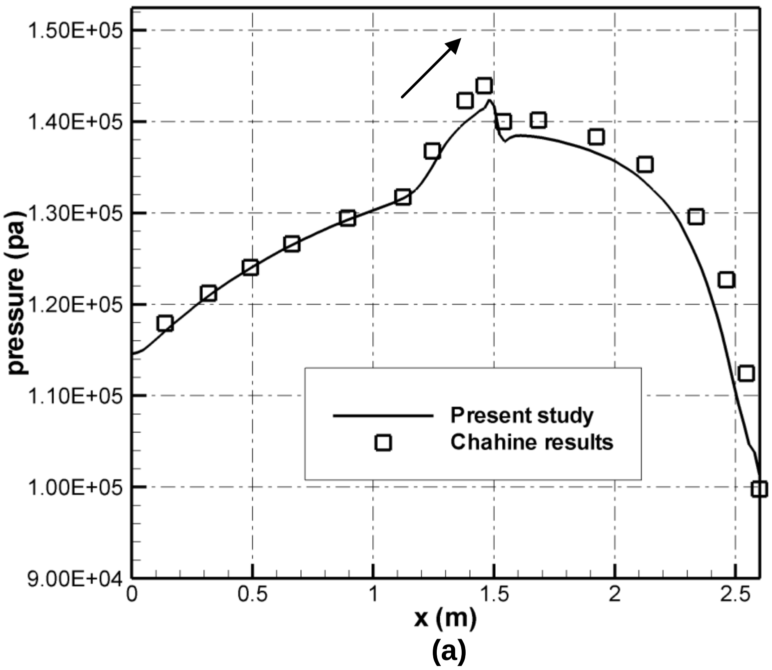

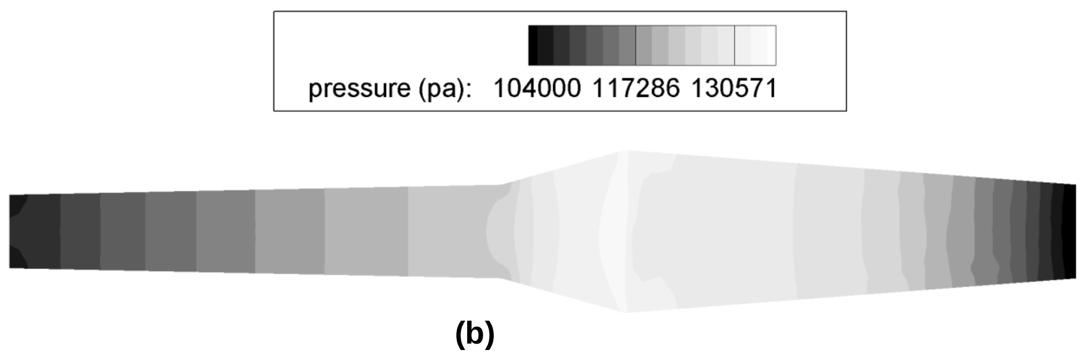

Figure 5. (a) Pressure distribution on the centerline; (b) Contour of pressure on center plane of ramjet.

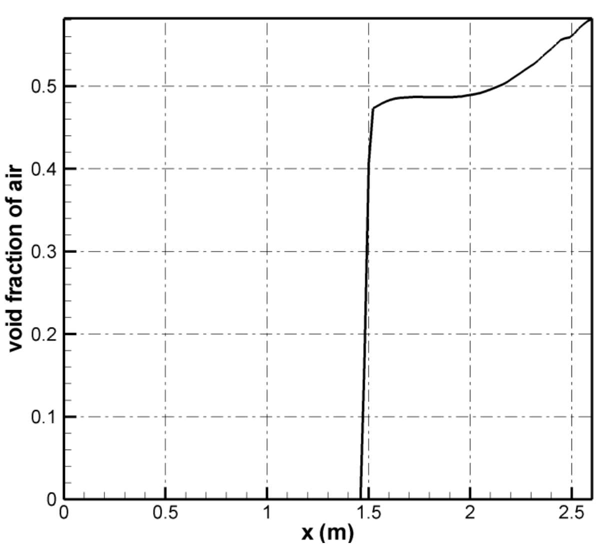

Figure 6. Void fraction variation in the ramjet.

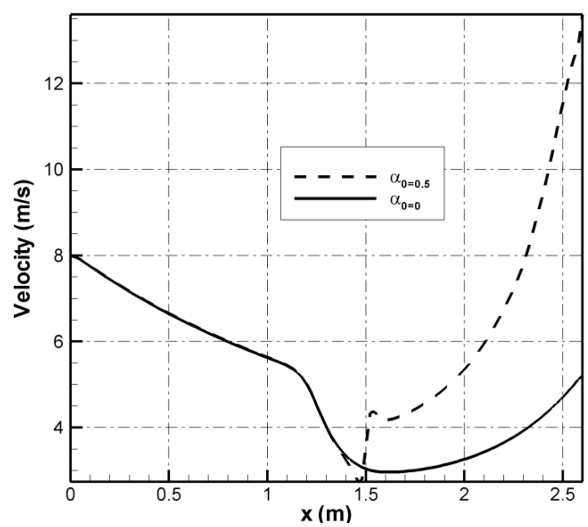

Figure 7. Velocity profile on the centerline for two different initial void fractions.

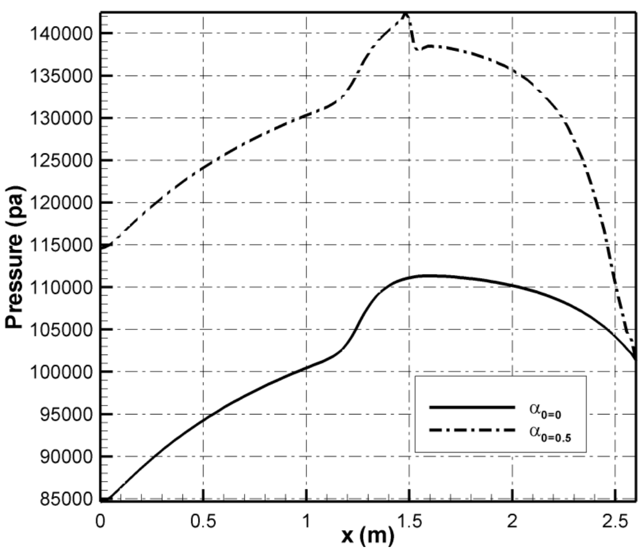

Figure 8. Pressure Distribution on the centerline for two different initial void fractions.

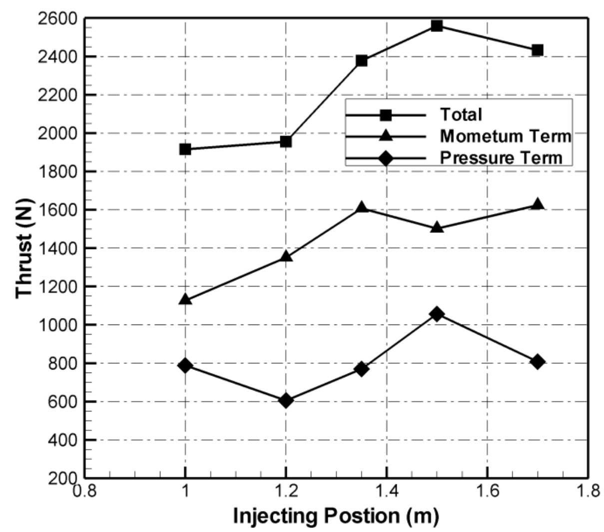

Figure 10. Effects of various bubbles injections positions on the computed thrust.

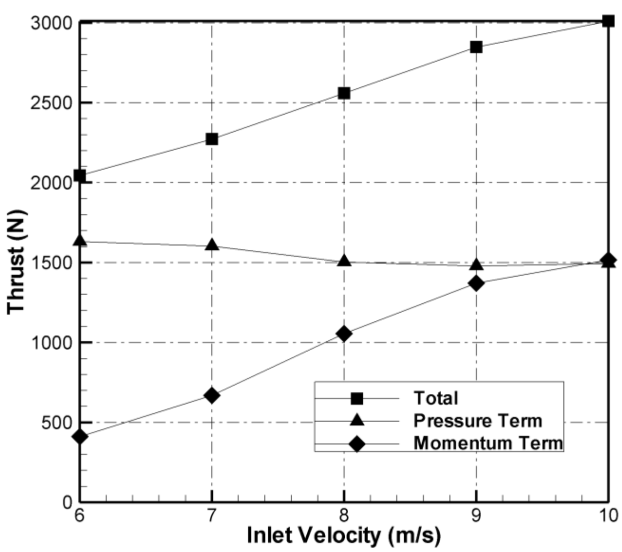

Figure 9. Thrust of the nozzle for different inlet velocities.

momentum flux over the surfaces of this control volume:

$$F_{Thrust} = (m^{\cdot}_e u_e - m^{\cdot}_i u_i) + (A_e P_e - A_i P_i) \quad (9)$$

The results for different inlet water velocities in the range of 6 to 10 m/s were computed. The predicted thrust from the 3-D model over a range of inlet velocities is depicted in Figure 9. As the inlet velocity increases, there is a large increment in the momentum contribution to the thrust, but a loss in the pressure component occurs. As a result, the total thrust increases as the inlet velocity increases.

To investigate the effects of the position of the injection point on thrust of the ramjet, five different locations have been considered. The results of this part are presented in Figure 10. The contribution of pressure term has more changes in comparison with its changes with the inlet velocity. It is observed that maximum thrust achieved when the injection occurs at the beginning of the nozzle.

In addition to the planar injection, injection from one point was also investigated. The affected zone of bubble injection is showed in Figure 11. The bubbles move only in the upper part of ramjet until they leave the ramjet.

Another way to improve the performance of the ramjet is changing the shape of diffuser. In this research a curved diffuser was also studied. The curve equation is given by Equation (10). The thrust for this type of ramjet was computed to be 3006.57 (N), which indicates that the curved diffuser increases thrust about 17.5%.

$$Y=-0.027x^3-0.009x^2-0.005x-0.076 \quad (10)$$

Conclusion

A three dimensional, time-averaged Navier-Stokes solver couppled with the Lagrangian equations for the bubble motions and time bubbbles radii variations have been used to simulate the flow field of a two-phase bubbly water flow of a ramjet with diverging-converging nozzle. The flow solver uses a finite volume approach. Validation results against an experimental two-phase water ramjet were presented and good agreement was observed. The effects of the various initial velocity of the incoming water on the performance and the thrust of the ramjet were inestigated. Results reveal that the increasing of the initial incoming velocity will increase the momentum parts of the thrust while decreasing the pressure parts, and

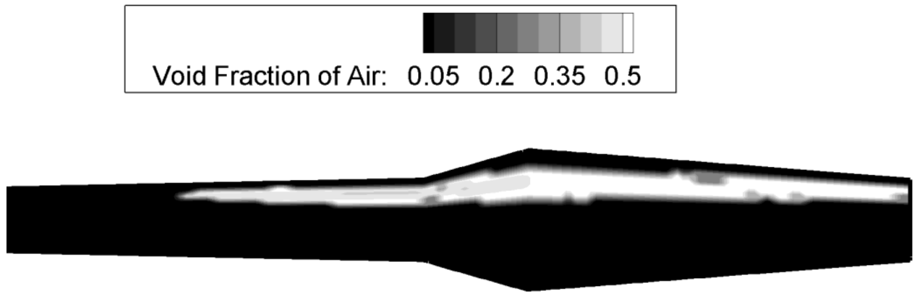

Figure 11. Contour of void fraction for injection from a point.

totally increase the thrust. Five different locations were used to implement the bubble injection and computed results showed that the bubble injection at the beginning nozzle section developed the highest thrust. Also it was shown that the ramjet thrust can be augmented by changing the difusser profile.

Conflict of Interest

The authors have not declared any conflict of interest.

Nomenclature:

Greek Symbols: A, Cross-sectional area {m^2); α. void fraction; C_D, Drag coefficient; α_0. initial void fraction; P_v, liquid vapor pressure (pa); μ.
Viscosity (N・s・m−2); P_{G0}, initial gas pressure (pa); ρ.Density (kg・m^{-3});
P, Pressure (pa); ν. Kinematic viscosity (m^2.s^{-1}); *R,* radius of bubble (m); γ,
Surface tension (N・m−1); R_0, reference bubble radius (m); δ_{ij}, Kronecker delta; *Re,* Reynolds number; T, temperature (K);
Indices: V, Volume (m^3); b, property of a bubble; d_{ij}, deformation tensor; n,
number of the bubble class; *g,* constant of gravity acceleration (m・s^{-2}); i,
Inlet; $m^{\cdot}$, mass rate (kg・s^{-1}); e, Exit; *t* , time (s); f, liquid phase; *u,* velocity (m・s^{-1}); m, mixture medium.

REFERENCES

Alehossein H, Qin Z (2007). Numerical analysis of Rayleigh-Plesset equation for cavitating water jets. Int. J. Num. Methods Eng. 72(7):780-807.

Amos RG, Maples G, Dyer DF (1973). Thrust of New York, USA: McGraw Hill, 1969. an air-augmented waterjet. J. Hydronautics 7(2):64-71.

Chahine GL (2008). Numerical Simulation of Bubble Flow Interactions. J. Hydrodynamics 21(3):316-332.

Chahine GL, Hsiao C, Choi J, Wu X (2008). Bubble Augmented Waterjet Propulsion: Two-Phase Model Development and Experimental Validation. 27th Symposium on Naval Hydrodynamics Seoul, Korea.

Fu Y, Wei Y, Zhang J (2009). Parametric study on the thrust of bubbly water Ramjet With a converging-diverging Nozzle. J. Hydrodynamics 21(5):591-599.

Haberman WL, Morton RK (1953). An experimental investigation of the drag and shape of air bubbles risingin various liquids. Report 802, DTMB.

Johnson VE, Hsieh T (1966). The influence of the trajectories of gas nuclei on cavitation inception. Sixth Symposium on Naval Hydrodynamics. pp. 163-179.

Maxwell TT, Maples G, Dyer DF (1975). Thrust of an air-augmented waterjet with a convergingdiverging nozzle. J. Hydronautics. 9(4):154-159.

Mor M, Gany A (2007). Performance mapping of bubbly water ramjet. Int. J. Maritime Eng. 149(A1):45-50.

Varshay H, Gany A (1997). Underwater two phase ramjet engine. United States Patent, 5692371.

Witte JH (1969). Predicted Performance of Large Water Ramjets. AIAA 2nd Advanced Marine Vehicles and Propulsion Meeting.Washington, USA: American Institute of Aeronautics and Astornautics Inc. pp. 3-47.


International Journal of Physical Sciences
Related Journals Published by Academic Journals
■African Journal of Pure and Applied Chemistry
■Journal of Internet and Information Systems
■Journal of Geology and Mining Research
■Journal of Oceanography and Marine Science
■Journal of Environmental Chemistry and Ecotoxicology
■Journal of Petroleum Technology and Alternative Fuels
academicJournals